SURFACTANT PROTEIN B (SP-B) ENHANCES THE CELLULAR SIRNA DELIVERY OF PROTEOLIPID COATED NANOGELS FOR INHALATION THERAPY

Pieterjan Merckx[a,1], *Lynn De Backer*[a,1], *Lien Van Hoecke*[b,c], *Roberta Guagliardo*[a], *Mercedes Echaide*[d], *Pieter Baatsen*[e], *Bárbara Olmeda*[d], *Xavier Saelens*[b,c], *Jésus Pérez-Gil*[d], *Stefaan C. De Smedt*[a], *Koen Raemdonck*[a,*]

[1] Both authors contributed equally to this work.

* Corresponding author.

Prof. Dr. Koen Raemdonck

Ghent Research Group on Nanomedicines
Laboratory of General Biochemistry and Physical Pharmacy
Faculty of Pharmaceutical Sciences
Department of Pharmaceutics
Ghent University
Ottergemsesteenweg 460, 9000 Ghent
Belgium

Telephone: +32 9 264 80 78
Fax: +32 9 264 81 89
Email: koen.raemdonck@ugent.be

[a] Ghent Research Group on Nanomedicines, Laboratory of General Biochemistry and Physical Pharmacy, Faculty of Pharmaceutical Sciences, Department of Pharmaceutics, Ghent University, Ottergemsesteenweg 460, 9000 Ghent, Belgium.

pieterjan.merckx@ugent.be; lynn.debacker@ugent.be; roberta.guagliardo@ugent.be; stefaan.desmedt@ugent.be

[b] VIB-UGent, Center for Medical Biotechnology, Technologiepark 927, 9052 Zwijnaarde (Ghent), Belgium.
[c] Department of Biomedical Molecular Biology, Ghent University, Technologiepark 927, 9052 Zwijnaarde (Ghent), Belgium.

lien.vanhoecke@vib-ugent.be; xavier.saelens@vib-ugent.be

[d] Departamento de Bioquímica y Biología Molecular, Facultad de Biologia, Research Institute Hospital 12 Octubre, Universidad Complutense, José Antonio Novais 12, 28040 Madrid, Spain.

mechaide@ucm.es; barbara_olmeda@bio.ucm.es; jperezgil@bio.ucm.es

[e] VIB-KU Leuven, VIB Bio Imaging Core, Center for Brain and Disease Research, Campus Gasthuisberg, Herestraat 49 box 602, 3000 Leuven, Belgium

pieter.baatsen@kuleuven.vib.be

ABSTRACT

Despite the many advantages of small interfering RNA (siRNA) inhalation therapy and a growing prevalence of respiratory pathologies, its clinical translation is severely hampered by inefficient intracellular delivery. To this end, we previously developed hybrid nanoparticles consisting of an siRNA-loaded nanosized hydrogel core (nanogel) coated with Curosurf®, a clinically used pulmonary surfactant (PS). Interestingly, the PS shell was shown to markedly improve particle stability as well as intracellular siRNA delivery *in vitro* and *in vivo*. The major aim of this work was to identify the key molecular components of PS responsible for the enhanced siRNA delivery and evaluate how the complexity of the PS coat could be reduced. We identified surfactant protein B (SP-B) as a potent siRNA delivery enhancer when reconstituted in proteolipid coated hydrogel nanocomposites. Improved cytosolic siRNA delivery was achieved by inserting SP-B into a simplified phospholipid mixture prior to nanogel coating. This effect was observed both *in vitro* (lung epithelial cell line) and *in vivo* (murine acute lung injury model), albeit that distinct phospholipids were required to achieve these results. Importantly, the developed nanocomposites have a low *in vivo* toxicity and are efficiently taken up by resident alveolar macrophages, a main target cell type for treatment of inflammatory pulmonary pathologies. Our results demonstrate the potential of the endogenous protein SP-B as an intracellular siRNA delivery enhancer, paving the way for future design of nanoformulations for siRNA inhalation therapy.

KEYWORDS

Surfactant Protein B, pulmonary surfactant, nanomedicines, RNA interference, siRNA, pulmonary delivery

1. INTRODUCTION

Pathologies of the respiratory tract are subject to a growing prevalence and for many of these illnesses an unmet therapeutic need exists. According to the latest report of the World Health Organization, chronic obstructive pulmonary disease, lower respiratory infections and lung cancer are among the top five leading causes of death worldwide. [1] To address this major global health problem, novel and efficient therapies are urgently needed.

Over the past two decades, research in the field of RNA interference (RNAi) has created new therapeutic opportunities. Activation of the RNAi pathway in the cytosol of affected cells, e.g. by small interfering RNA (siRNA), enables the specific post-transcriptional silencing of key molecular disease targets. As the expression of virtually all genes is susceptible to silencing by siRNAs, new therapeutic targets have emerged that are not readily druggable by conventional small molecules. [2],[3] The lung is an attractive target organ for siRNA therapeutics, since it offers the possibility for non-invasive local administration. Inhalation therapy with siRNA (i) enables direct and prolonged contact with pulmonary cells, (ii) limits systemic exposure, (iii) lowers the required therapeutic dose and (iv) allows for self-administration, resulting in a better patient compliance. [4] Unfortunately, despite these advantages, still many extra- and intracellular barriers limit the siRNA dose that effectively reaches the cytosol of the target cells. [5] To guide siRNA across these biological barriers, many research groups attempt to formulate siRNA into *synthetic* polymer- or lipid-based nanoparticles (NPs).

However, such NPs often fail to merge efficient siRNA delivery with biocompatibility, [6-8] rationalizing the growing interest in the application of *bio-inspired* materials for drug delivery. In this context, we recently reported on hybrid NPs composed of an siRNA-loaded polymeric matrix core that is coated with a proteolipid shell of Curosurf®, a clinical pulmonary surfactant (PS). [9],[10] The core of these NPs consists of a cationic polysaccharide hydrogel nanoparticle (nanogel; NG), which has a high loading capacity for siRNA (~0.4 µg/µg) and a proven delivery potential in various cell types. [11-13] PS is an endogenous surface-active material that covers the alveolar surface to maintain a low surface tension upon expiration and prevent alveolar collapse. In the context of siRNA delivery, PS is primarily regarded as an important extracellular barrier in the deep lung that limits access to underlying cells upon inhalation therapy. [14],[15] Nonetheless, we observed that a PS outer layer around siRNA loaded NGs (siNGs), although hampering cellular uptake, significantly enhanced intracellular siRNA delivery in lung cell types *in vitro* and *in vivo* (**Scheme S1**). However, the molecular determinants for this delivery-

promoting effect remain elusive. [9],[10] Native PS is composed of various lipids (~90 wt%) and specialized surfactant proteins (SPs, ~10 wt%). [16] The lipid fraction mainly consists of phosphatidylcholine (PC) (~60-70 wt%) and anionic phospholipids such as phosphatidylglycerol (PG) and phosphatidylinositol (~10-15 wt%) species. Among PC lipids, 1,2-dipalmitoyl-*sn*-glycero-3-phosphocholine (DPPC) represents ~40-50 wt% of the total surfactant mass. DPPC is essential to sustain the required low surface tension during expiration. The negatively charged PG is believed to promote interaction with surfactant protein B (SP-B) and surfactant protein C (SP-C), both cationic and hydrophobic. Although required for the endogenous biological activity of pulmonary surfactant, we hypothesize that many of these components are redundant in the context of cellular delivery of siRNA. Therefore, the aim of this work was to identify the key constituents in PS that are responsible for the enhanced cytosolic siRNA delivery. Hereto, siNGs were layered with a PS-inspired proteolipid coat of varying composition. The impact on siRNA delivery was tested both *in vitro* in non-small cell lung cancer cells (H1299) and *in vivo* in a murine lipopolysaccharide-induced acute lung injury model, using an siRNA to target tumor necrosis factor (TNF) α. We found that the siRNA delivery promoting effect was governed by SP-B, for which the extent of the effect depends on the phospholipid environment in which it is embedded. This knowledge could serve as a basis for future rational design of novel pulmonary siRNA delivery platforms.

2. MATERIALS & METHODS

2.1. Small interfering RNAs

For *in vitro* experiments, 21 nucleotide (nt) small interfering RNA (siRNA) duplexes targeted against Enhanced Green Fluorescent Protein (eGFP), hereafter abbreviated as siEGFP and non-targeting negative control duplexes (siCTRL), were purchased from Eurogentec (Seraing, Belgium). For siEGFP: sense strand = 5´-CAAGCUGACCCUGAAGUUCtt-3´; antisense strand = 5´-GAACUUCAGGGUCAGCUUGtt-3´. For siCTRL: sense strand = 5´-UGCGCUACGAUCGACGAUGtt-3´; antisense strand = 5´-CAUCGUCGAUCGUAGCGCAtt-3´ (capital letters represent ribonucleotides; lower case letters represent 2´-deoxyribonucleotides). For fluorescence experiments, the siCTRL duplex was labeled with a Cy®5 dye at the 5' end of the sense strand (siCy5). The fluorescent modifications were performed and verified by Eurogentec. The concentration of the siRNA stock solutions in nuclease-free water (Ambion®-Life Technologies, Ghent, Belgium) was calculated from absorption measurements at 260 nm (1 OD_{260} = 40 µg/mL) with a Nanodrop 2000 spectrophotometer (Thermo Fisher Scientific, DE, USA). For *in vivo* experiments, stabilized 21 nt siRNA duplexes (siSTABLE), targeted against murine tumor necrosis factor (TNF) α, hereafter abbreviated as siTNFα, and non-targeting negative control duplexes (siCTRL) were purchased from GE Healthcare Dharmacon (Diegem, Belgium). The used siTNFα was selected from a set of four proposed sequences as provided by the manufacturer, by testing TNFα knockdown for all sequences *in vitro* (**Figure S1**) using the TNF alpha Ready-SET-Go!® ELISA assay (eBioscience, San Diego, CA, USA). siTNFα sense strand = 5'-CAAAUGGCCUCCCUCUCAUUU-3'; antisense strand = 5'-AUGAGAGGGAGGCCAUUUGUU-3'. The sequence of stabilized siCTRL was confidential and could not be listed.

2.2. Synthesis of dextran nanogels and loading with siRNA

Cationic dextran nanogels were prepared using an inverse miniemulsion photopolymerization method as reported previously. [11] Briefly, 150 mg of dextran hydroxyethyl methacrylate (dex-HEMA) with a degree of substitution of 5.2 [33] was dissolved in a solution containing 97.5 µL Irgacure 2959 (10 mg/mL in water; Sigma-Aldrich, Bornem, Belgium) as UV curing photoinitiator, 180 µL nuclease-free water and 195 µL of a cationic methacrylate monomer, [2-(methacryloyloxy)-ethyl] trimethylammonium chloride (TMAEMA, 80 wt% solution in water; Sigma-Aldrich). The obtained dex-HEMA solution was

emulsified in 5 mL of mineral oil (Sigma-Aldrich), supplemented with the surfactant ABIL EM 90 (0.5 mL) (Evonik Goldschmidt GmbH, Essen, Germany), through ultrasonication (90 s, amplitude 15 %; Branson Digital Sonifier®, Danbury, USA). The formed emulsified nanodroplets were immediately cross-linked by UV irradiation (900 s, Bluepoint 2.1 UV source, Hönle UV technology, Gräfelfing, Germany) under cooling (4 °C). The resulting dex-HEMA-*co*-TMAEMA nanogels, hereafter abbreviated as NGs, were collected by precipitation in acetone and washed 4 times with acetone:hexane (1:1). Traces of organic solvent were removed by vacuum evaporation and the pellet was redispersed in 5 mL nuclease-free water. To assure long-term stability, the NGs were lyophilized and stored desiccated. To obtain siRNA-loaded NGs (siNGs) for *in vitro* experiments, a NG stock (2 mg/mL) was prepared by dispersing a weighed amount of lyophilized particles in ice-cooled nuclease-free water, followed by brief sonication (3 x 5 s, amplitude 10 %; Branson Digital Sonifier®, Danbury, USA). Subsequently, equal volumes of NG and siRNA dilutions in 4-(2-hydroxyethyl)-1-piperazineethanesulfonic acid (HEPES) buffer (pH 7.4, 20 mM) were mixed and incubated at 4 °C for ≥ 15 min to allow electrostatic complexation. For *in vivo* experiments, a NG stock (10 mg/mL) was prepared as described above. The NG stock contained less than 0.5 EU/mL lipopolysaccharide (LPS) as determined by the Endosafe®-PTS™ assay (Charles River International, Lecco, Italy). NGs and siRNAs were diluted in nuclease-free water prior to mixing and incubation. In addition, all preparative steps for the *in vivo* experiments were performed with LPS-free materials under LPS-free conditions. The concentration of siRNA dilutions used for NG loading was adjusted according to the intended dose.

2.3. Isolation, analysis and quantification of hydrophobic surfactant proteins

The isolation of SP-B and SP-C from native porcine pulmonary surfactant or Curosurf® (a commercially available porcine pulmonary surfactant preparation; Chiesi Farmaceutici, Parma, Italy) was performed as described earlier by Pérez-Gil and coworkers. [34] For extraction from native porcine lungs, the lungs were first minced and carefully washed. Next, the mixture was filtered and centrifuged (1000 g at 4 °C for 15 min). The supernatant was again centrifuged (3000 g at 4 °C for 2 h) and from the isolated pellet, enriched in large lipid/protein PS complexes, the hydrophobic components including lipids and hydrophobic surfactant proteins were extracted with chloroform/methanol mixtures according to the Bligh & Dyer method. Chromatographic separation in Sephadex LH-20 (GE Healthcare, Machelen, Belgium) of the organic extract allowed separating the hydrophobic protein fraction from the surfactant lipid fractions. A subsequent chromatographic step in Sephadex LH-60 yielded purification of

SP-B and SP-C, which were stored in chloroform/methanol solutions. Phospholipid contamination of the protein samples was quantified by phosphorus determination as described by Rouser *et al*. [35] Purity and nature of isolated pools of proteins were analyzed by sodium dodecyl sulfate (SDS) electrophoresis in polyacrylamide gels and subsequent western blot with anti-SP-B and anti-SP-C primary antibodies (Seven Hills, Cincinnati, OH, USA). The quantification of the amount of isolated SP-B and SP-C was performed by an amino acid analysis.

2.4. Preparation of Curosurf® coated siRNA-loaded nanogels

Prior to the formation of the Curosurf® pulmonary surfactant coat, the NGs were loaded with siRNA, as described above. The unprocessed Curosurf® dispersion (80 mg/mL) was diluted to 4.5 mg/mL in HEPES buffer and incubated with siNGs in equal volumes for 10 min at 4 °C, using a Curosurf® to NGs weight ratio of 15 mg/mg. Subsequently, the surfactant coat on the siNGs was formed by sonication (3 x 10 s, amplitude 10 %; Branson Digital Sonifier®, Danbury, USA). This resulted in a hybrid nanoparticle as described earlier, [9] further denoted as Curosurf® coated siNGs.

2.5. Preparation of proteolipid coated siRNA-loaded nanogels

The following phospholipids were used for siNG coating: 1,2-dipalmitoyl-*sn*-glycero-3-phosphocholine (DPPC), 1-palmitoyl-2-oleoyl-*sn*-glycero-3-phosphocholine (POPC), L-α-phosphatidylglycerol (eggPG), and 1,2-dioleoyl-*sn*-glycero-3-phosphocholine (DOPC). All phospholipids were purchased from Avanti Polar Lipids, Inc. (AL, USA). The phospholipids were mixed in chloroform at different weight ratios, specified in every figure caption and listed in **Table S1**. In order to incorporate SP-B and/or SP-C in the phospholipid outer layer, the isolated hydrophobic proteins were combined with the phospholipids in chloroform at indicated concentrations. A (proteo)lipid film was formed by rotary evaporation of the organic solvent under vacuum at 37 °C. The dried (proteo)lipid film was rehydrated in HEPES buffer by mechanical agitation, resulting in a final (proteo)lipid concentration of 4.5 mg/mL. The hydrated (proteo)lipid film was used in the coating procedure, as described above, for which the ratio of the (proteo)lipid mixture to NGs was 15 mg/mg (*in vitro* experiments) or 10 mg/mg (*in vivo* experiments). The (proteo)lipid-siNG mixtures for *in vivo* administration were diluted 2-fold in nuclease-free water prior to sonication. This resulted in a hybrid nanoparticle further denoted as proteolipid coated siNGs. Hydrodynamic diameter and zeta-potential of all formulations were determined

via Dynamic Light Scattering (DLS) (Zetasizer Nano, Malvern Instruments, Worcestershire, United Kingdom). All formulations were imaged using transmission electron cryomicroscopy (cryoTEM). 3.5 µL of every sample was applied to a 300 mesh quantifoil grid (1/3.5) and incubated for 30 s. Next, grids were mounted in a plunge-freezer (EMBL), blotted one-sided for 3 s using a Whatman 1 filter paper and plunged into liquid ethane at a temperature of −180 °C, followed by storage in liquid nitrogen until observation. Next, the samples were transferred to a Gatan 914 cryoholder and imaged at low dose conditions at −177 °C, using a JEOL JEM1400 TEM equipped with an 11 Mpxl Olympus SIS Quemesa camera. All formulations were checked for cytotoxicity by a CellTiter-Glo® assay (Promega, Leiden, The Netherlands) prior to uptake and silencing experiments.

2.6. Cell line and culture conditions

Cell culture experiments were performed using a human lung epithelial cell line (H1299) that stably expresses eGFP (H1299_eGFP), obtained from the lab of Prof. Camilla Foged (Department of Pharmacy, University of Copenhagen, Denmark). H1299_eGFP cells were cultured in RPMI 1640 supplemented with 2 mM glutamine, 10 % fetal bovine serum and 100 U/mL penicillin/streptomycin at 37 °C in a humidified atmosphere containing 5 % CO_2. Cells were passaged every 3 days using 0.25 % trypsin-ethylenediaminetetraacetic acid (EDTA) solution in order to maintain sub-confluency. H1299_eGFP cells were treated with medium containing 1 mg/mL Geneticin® once per month for eGFP transgene selection. All materials were purchased from Gibco®-Life Technologies (Grand Island, NY, USA), except for the serum, which was delivered by Hyclone™ (GE Healthcare, Machelen, Belgium).

2.7. Quantification of *in vitro* cellular siRNA internalization in H1299_eGFP cells by flow cytometry

To quantify the cellular uptake of siRNA by flow cytometry, H1299_eGFP cells were seeded in 24-well plates (Greiner Bio-One GmbH, Kremsmünster, Austria) at a density of 2 x 10^4 cells/cm^2 and left to settle overnight. NGs were loaded with different amounts of siCTRL:siCy5 (100:0.75 mol%) and coated with Curosurf® or a proteolipid mixture using the coating procedure described above. After 5-fold dilution in Opti-MEM® (final NG concentration of 30 µg/mL), the particles were incubated with the cells for 4 h (37 °C, 5 % CO_2). Following incubation, the cells were washed with dextran sulfate sodium salt (0.1 mg/mL in PBS) to remove cell surface-bound fluorescence. Next, the cells were harvested by

trypsinization (trypsin/EDTA 0.25 %), resuspended in 250 µL flow buffer (PBS supplemented with 1 % bovine serum albumin and 0.1 % sodium azide) and incubated on ice until flow cytometry analysis. Transfections were performed in technical triplicate per independent biological repeat and a minimum of 10^4 cells was analyzed in each measurement, using a FACSCalibur™ flow cytometer (BD Biosciences, Erembodegem, Belgium). Data analysis was performed using the FlowJo™ analysis software (Treestar, Costa Mesa, USA).

2.8. Quantification of *in vitro* eGFP silencing in H1299_eGFP cells by flow cytometry

H1299_eGFP cells were seeded in 24-well plates (Greiner Bio-One GmbH; 1.85 x 10^4 cells/cm^2). NGs were loaded with variable amounts of siCTRL or siEGFP. Next, the siNGs were coated with Curosurf® or a proteolipid mixture using the coating procedure described above. After 5-fold dilution in Opti-MEM® (final NG concentration of 30 µg/mL), the particles were incubated with the cells for 4 h (37 °C, 5 % CO_2). Following incubation, non-internalized nanoparticles were washed away with PBS and the cells were incubated with 1 mL fresh cell culture medium for 48 h. The cells were then prepared for analysis by flow cytometry as described above. Transfections were performed in technical triplicate per independent biological repeat and a minimum of 2 x 10^4 cells was analyzed in each measurement as described above.

2.9. *Ex vivo* quantification of siRNA uptake by different immune cell types and assessment of acute *in vivo* toxicity and cellular influx in naive BALB/c mice

Female BALB/c mice were purchased from Charles River Italy and housed under specific pathogen-free conditions in individually ventilated cages in a controlled 12 h day-night cycle and given food and water *ad libitum*. All mice were 8 weeks old at the start of the experiments. All procedures involving animals were approved by the local Ghent University ethics committee (accreditation nr. LA1400536, Belgium), in accordance with European guidelines. The (proteolipid coated) siNGs and control suspensions for administration were prepared as described above, followed by a 2-fold dilution in 2 times concentrated PBS. Per mouse, a dose of 100 µg NG loaded with 1 pmol siCy5 per µg NG was administered. Mouse tracheal aspiration was used for NP administration. [36] Briefly, after sedation with isoflurane (inhalation at 4 % for induction and 3 % for maintenance), individual mice were placed in a near-vertical position. The animal's tongue was extended with lined forceps, and 80 µL of the NP

suspension was instilled posterior of the pharynx. The tongue was held in position until the dispersion was inhaled into the lungs. Control mice were administered 80 µL of PBS. 24 h after NP administration, bronchoalveolar lavage (BAL) isolation was performed as described by Van Hoecke *et al*. [37] The mice were euthanized by intraperitoneal injection of a lethal dose of Nembutal® (pentobarbital, 200 mg/kg in PBS; Ceva, Brussels, Belgium). Immediately after euthanization, a lavage cannula was placed into the trachea through a small incision. The lungs were flushed once with 1 mL Ca^{2+}- and Mg^{2+}- free Hank's balanced salt solution (HBSS; Invitrogen™-Life Technologies), supplemented with 0.05 mM EDTA (Sigma-Aldrich). The obtained BAL was subsequently centrifuged (400 g, 7 min, 4 °C), to separate the cellular fraction from the supernatant. The BAL cellular fraction was resuspended in PBS. The different cell types isolated from the BAL fluids were typed and quantified by flow cytometry. Fc-blocked (1 µg/ml; clone 2.4G2; BD Biosciences, San Jose, CA, USA) cells were stained with anti-mouse major histocompatibility complex (MHC) class II-eFluor 450 (0.4 µg/mL, clone M5/114.15.2; eBioscience, San Diego, CA, USA), CD3ε-Alexafluor 488 (1 µg/mL, clone245-2C11; BD Biosciences), SiglecF-phycoerythrin (1 µg/mL, clone E50-2440; BD Biosciences), CD4-peridinin-chlorophyll protein complex 5 (1 µg/mL, clone RM4-5; BD Biosciences), CD8-PE-Cy®7 (1 µg/mL, clone 53-6.7; BD Biosciences), CD11b-allophycocyanin-Cy®7 (1 µg/mL, clone M1/70; BD Biosciences). A live-dead staining was added to exclude dead cells from the analysis. All samples were measured on a FACS LSRII flow cytometer (BD Biosciences) and acquired using FACSDiva software (BD Biosciences). Within the single cells that were alive, $CD4^+$ and $CD8^+$ T lymphocytes were identified as $CD3\varepsilon^+CD4^+$ and $CD3\varepsilon^+CD8^+$ cells, respectively. Alveolar macrophages were identified within the $CD3\varepsilon^-Cd11c^+$ cell population based on their high expression of Siglec-F. Finally neutrophils and eosinophils were identified as $CD3\varepsilon^-CD11c^-$ $Siglec\text{-}F^-CD11b^+$ and $CD3\varepsilon^-CD11c^-Siglec\text{-}F^+CD11b^+$ cells respectively in the remaining cell population. Data analysis was performed using the FlowJo™ analysis software (Treestar, Costa Mesa, USA). The BAL supernatant was quantified for murine interleukin 1α (IL-1α), interleukin 1β (IL-1β), granulocyte-macrophage colony-stimulating factor (GM-CSF), interleukin 6 (IL-6), tumor necrosis factor α (TNFα), macrophage inflammatory protein 1α (MIP-1α), KC and monocyte chemoattractant protein 1 (MCP-1) with a Bio-Plex® Suspension array system (Biorad, Hercules, USA) according to manufacturer's specifications. The analytes were measured with a Luminex protein array reader and Bio-Plex® manager software version 5.0 (Bio-Rad Laboratories), using recombinant standards (Bio-Rad Laboratories). For data analysis, a 5-parameter logistic curve fit was applied to each standard curve and sample. In

addition, the supernatant was quantified for mouse albumin using a Mouse Albumin ELISA Kit (Genway Biotech, San Diego, CA, USA).

2.10. *In vivo* TNFα silencing in murine acute lung injury (ALI) model

Female BALB/c mice were purchased from Charles River Italy and kept in the same conditions as described above. The (proteolipid-coated) siNGs and control suspensions for administration were prepared as described above, followed by a 2-fold dilution in 2 times concentrated PBS. Per mouse, a dose of 100 µg NG loaded with 1 pmol TNFα targeting siRNA (siTNFα) or siCTRL per µg NG was administered. Mouse tracheal aspiration [36] was used for NP administration as described above. 24 h after NP administration, mice received a lipopolysaccharide (LPS) dose of 5 µg in 80 µL PBS *via* tracheal aspiration. [36] 48 h after NP administration, thus 24 h after LPS administration, BAL isolation [37] was performed. The obtained BAL was subsequently centrifuged (400 g, 7 min, 4° C), to separate the cellular fraction from the supernatant. The BAL supernatant was quantified for murine TNFα with a Bio-Plex® Suspension array system (Biorad, Hercules, USA) as previously described.

2.11. Statistical analysis

All *in vitro* experiments were performed in technical triplicate and as 3 independent biological repeats (n=3), unless otherwise stated. All *in vivo* experiments were performed as 4 biological replicates (n=4). All data are presented as mean ± standard deviation (SD). Statistical analysis was performed *via* One-way ANOVA followed by a Tukey's multiple comparison test, using GraphPad Prism software version 6. Error bars for *in vivo* silencing represent standard error of mean (SEM).

3. RESULTS AND DISCUSSION

3.1. Identification of Curosurf® components responsible for enhanced siRNA delivery

We recently reported on the unanticipated finding that the decoration of siRNA-loaded dextran nanogels (siNGs) with a clinically used pulmonary surfactant (PS) from porcine origin (Curosurf®) substantially enhanced cellular siRNA delivery both *in vitro* [9] and *in vivo*. [10]

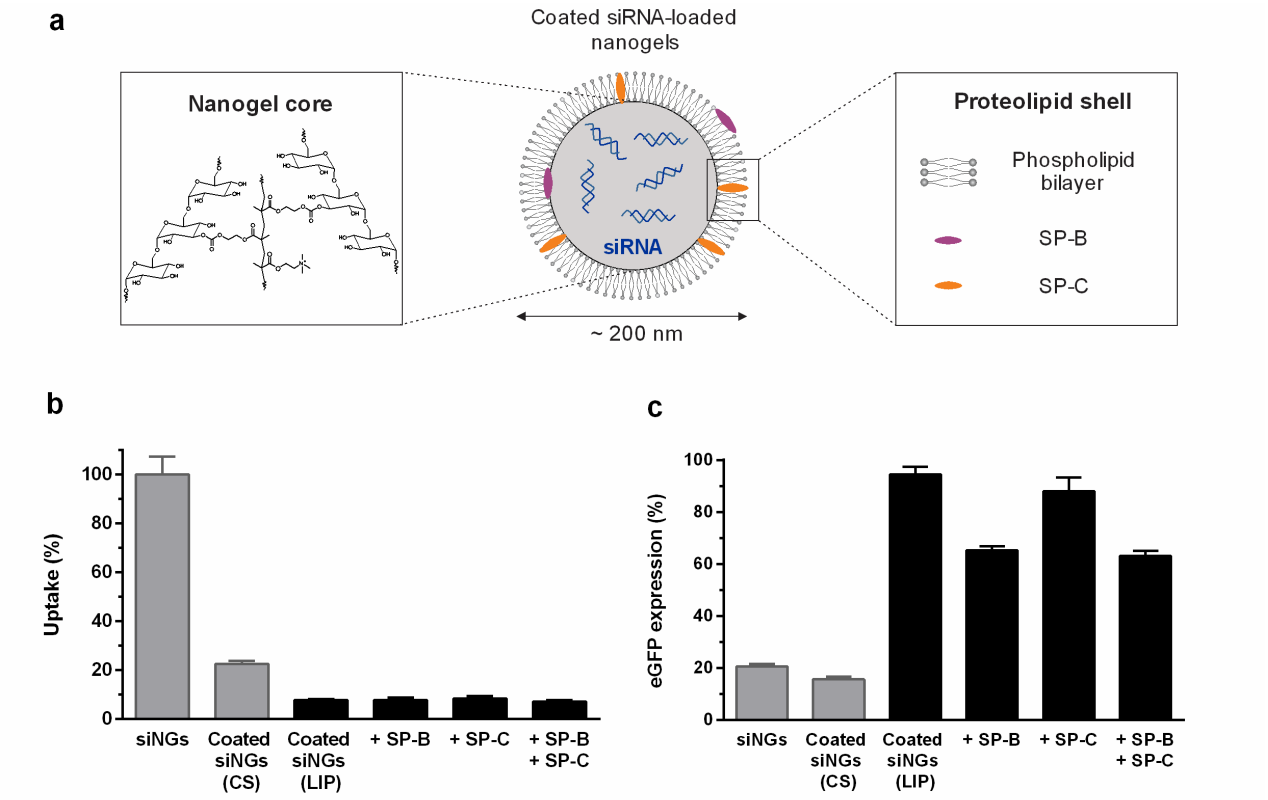

Figure 1. Biological activity of siNGs coated with surfactant protein containing proteolipid mixtures. (a) Schematic illustration of the (proteo)lipid coated siRNA-loaded nanogels (siNGs). Evaluation of **(b)** cellular uptake and **(c)** gene silencing potential of siNGs in H1299_eGFP cells determined *via* flow cytometry. The siNGs were layered with Curosurf® (coated siNGs (CS)) or DPPC:POPC:eggPG (50:35:15 wt%; coated siNGs (LIP)). In this LIP outer layer, SP-B (0.4 wt%) and/or SP-C (0.7 wt%) were incorporated. In the uptake experiments, NGs were loaded with fluorescently labeled control siRNA (siCy5), for which values of the coated formulations are shown relative to the maximal amount of particles taken up, i.e. for uncoated siNGs (100 %). The eGFP expression of the cells treated with eGFP-targeting siRNA (siEGFP) was normalized to the expression of cells treated with control siRNA (siCTRL). All experiments were performed with a fixed NG concentration (30 µg/mL) and siRNA concentration (50 nM) (technical triplicate).

Comparable to native human PS, the most abundant component of the (phospho)lipid fraction in Curosurf® is 1,2-dipalmitoyl-*sn*-glycero-3-phosphocholine (DPPC), representing ~40-50 wt% of the total surfactant mass. Other important phospholipids include (unsaturated) PCs and the anionic phosphatidylglycerol (PG). In contrast to native human PS, cholesterol is removed during production of Curosurf®, as well as the hydrophilic surfactant proteins (SPs), *i.e.* SP-A and SP-D. [17]

To evaluate the contribution of the remaining hydrophobic SPs to the PS-enhanced siRNA delivery, siNGs were initially coated with a mixture of abundant PS phospholipids, *i.e.* DPPC, 1-palmitoyl-2-oleoyl-*sn*-glycero-3-phosphocholine (POPC) and L-α-phosphatidylglycerol (eggPG) in a 50:35:15 weight ratio. This synthetic lipid mixture was supplemented with SP-B and/or SP-C isolated from Curosurf®, using weight ratios documented in the literature (*i.e.* 0.4 wt% SP-B and 0.7 wt% SP-C) (**Figure 1a**). [18]

As illustrated in **Figure 1b**, the presence of either a Curosurf® or simplified (proteo)lipid outer layer markedly reduced the uptake of siNGs in lung epithelial cells (H1299_eGFP), which was most pronounced for the synthetic compositions. Remarkably and in agreement with our earlier observations, [9] Curosurf® (CS) coated siNGs retained their gene silencing potential, despite the lower uptake. However, in the absence of SPs (i.e. siNGs coated with the DPPC:POPC:eggPG (LIP) mixture only) and in line with earlier data using CS as coating material, [19] this impaired cellular internalization also abrogated the gene silencing potential of the siNGs (**Figure 1c**). Interestingly, despite a similar reduction in cellular siRNA uptake, the addition of 0.4 wt% SP-B resulted in 40 % eGFP gene suppression, an effect that could not be mimicked by SP-C. Although the extent of eGFP silencing obtained by the Curosurf® coating could not be reached, these pilot data clearly suggest that SP-B is a key molecular determinant for the enhanced siRNA delivery effects initially observed earlier for Curosurf®. [9] This finding is more thoroughly investigated in the experiments below.

3.2. Impact of lipid composition on SP-B functionality

As it is known that the hydrophobic SP-B and SP-C preferentially localize in a liquid state lipid environment, we compared the efficiency of siNGs layered with DPPC:eggPG (85:15 wt%) or DOPC:eggPG (85:15 wt%) (**Figure 2**). These binary phospholipid mixtures are a combination of the negatively charged eggPG, required for coating of the cationic siNGs *via* electrostatic interaction, with a fully saturated (DPPC, phase transition temperature (T_m) = 41°C) or unsaturated (DOPC, T_m = -17°C) phosphatidylcholine (PC). All coated formulations have an average size <200 nm, a zeta-potential < -20 mV and a PDI <0.25, indicating colloidal stability (**Figure S2**). In addition, transmission electron cryomicroscopy (cryoTEM) imaging confirmed the anticipated core-shell morphology (**Figure S3**). As expected, independent of both the applied phospholipid mixture and the presence of SP-B, the cellular internalization of siNGs was markedly reduced after coating (>90 %) (**Figure 2a**). The latter resulted in negligible gene knockdown in the absence of SP-B (**Figure 2b**).

However, supplementing the DPPC:eggPG coat with SP-B (0.8 wt%) generated a similar level of knockdown compared to the previous results on DPPC:POPC:eggPG (**Figure 1c**).

Analogous to the data presented in **Figure 1**, the addition of SP-C to the DOPC:eggPG coat did not improve eGFP silencing and thus siRNA delivery (**Figure 3**), confirming that, independent of the saturation level of the phospholipid coat, SP-B is responsible for the enhanced cytosolic delivery of siRNA. From a biophysical point of view, SP-B is essential to maintain proper lung function by promoting lipid adsorption onto the alveolar air-liquid interface and stabilization of multilamellar surfactant films during expansion-compression breathing cycles. [22, 23]

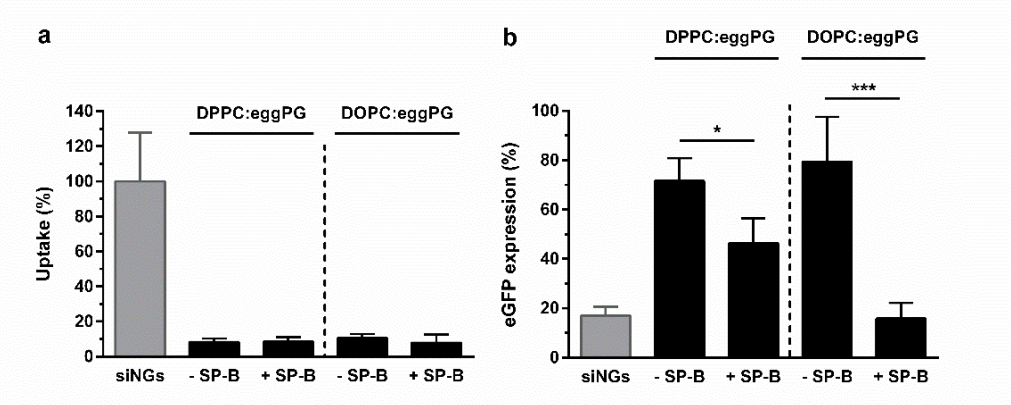

Figure 2. Impact of the main phospholipid in the outer proteolipid layer on siNGs biological activity. Evaluation of **(a)** cellular uptake and **(b)** gene silencing potential of siNGs in H1299_eGFP cells determined *via* flow cytometry. The siNGs were layered with DPPC:eggPG (85:15 wt%) or DOPC:eggPG (85:15 wt%) in the absence or presence of SP-B (0.8 wt%). In the uptake experiments, NGs were loaded with fluorescently labeled control siRNA (siCy5), for which values of the coated formulations are shown relative to the maximal amount of particles taken up, i.e. for uncoated siNGs (100 %). The eGFP expression was normalized to the expression of cells treated with control siRNA (siCTRL). All experiments were performed with a fixed NG concentration (30 µg/mL) and siRNA concentration (50 nM) (n=2; * $p \leq 0.05$, *** $p \leq 0.001$).

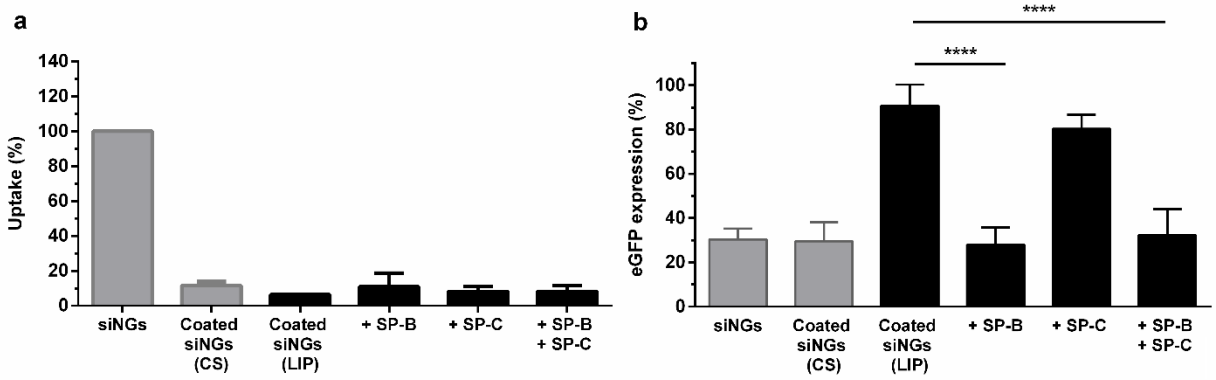

Figure 3. Biological activity of siNGs coated with a DOPC:eggPG mixture supplemented with different surfactant protein combinations. Evaluation of **(a)** cellular uptake and **(b)** gene silencing potential of siNGs in H1299_eGFP cells determined *via* flow cytometry. The siNGs were layered with Curosurf® (coated siNGs (CS)) or DOPC:eggPG (85:15 wt%; coated siNGs (LIP)). In this LIP outer layer, SP-B (0.4 wt%) and/or SP-C (0.7 wt%) were incorporated. In the uptake experiments, NGs were loaded with fluorescently labeled siRNA (siCy5), for which values of the coated formulations are shown relative to the maximal amount of particles taken up, i.e. for uncoated siNGs (100 %). The eGFP expression was normalized to the expression of cells treated with control siRNA (siCTRL). All experiments were performed with a fixed NG concentration (30 µg/mL) and siRNA concentration (50 nM) (n=3). For silencing experiments with SP-C alone n=2 (**** $p \leq 0.0001$).

It is believed that this interfacial activity is linked to both SP-B's fusogenic properties and its ability to facilitate close contact between neighboring membranes. The presence of SP-B in the surfactant outer shell of the nanocomposites might therefore induce fusion of the outer layer with the target cell plasma membrane and/or endolysosomal membrane, thus improving cytosolic siRNA delivery. [20, 21]

Remarkably, replacing the rigid DPPC by the more fluid DOPC significantly promoted gene silencing, this time reaching comparable levels of knockdown as measured for uncoated siNGs (**Figure 2b**), albeit with a minor reduction in cell viability (**Figure S4**). It is conceivable that a more fluid state (phospho)lipid crystalline environment in the particle coat might further facilitate SP-B mediated intermembrane interactions, given a less dense phospholipid packing and thus less resistance for lateral diffusion in the membrane. In addition, a recent model has suggested that SP-B organizes in the form of supramolecular multimers to support its function (e.g. membrane fusion), which also likely requires lateral mobility in its (phospho)lipid environment. [24] Possibly, these multimers are also important for siRNA delivery. Unraveling the mechanism of action of SP-B will be the subject of future investigations.

3.3. Evaluation of SP-B from different origins and impact of SP-B concentration

To further validate the key role of SP-B, we tested different batches of SP-B, *i.e.* isolated from Curosurf® or freshly extracted porcine lungs (n=3). Independent of the source, the inclusion of SP-B in the DOPC:eggPG outer layer similarly reduced the cellular internalization but maintained the gene silencing potential of the proteolipid coated siNGs in H1299_eGFP cells, which underscores the validity of our findings (**Figure 4a** and **4b**). In this context, we also investigated if we could amplify the effect by increasing the concentration of SP-B. Higher fractions of SP-B in the outer lipid layer seemed to further reduce cellular uptake of siRNA by the H1299_eGFP cells. Hence, the gene silencing potential was also slightly less pronounced. Nevertheless, even at 1.6 wt% SP-B, 60 % eGFP silencing is obtained with 10 nM of siRNA despite the ~25-fold reduction in cellular siRNA dose relative to uncoated siNGs (**Figure 4e** and **4f**). Also, when decreasing the SP-B fraction in the proteolipid coat, a significant reduction in eGFP knockdown was observed at 0.1 wt% of SP-B (**Figure 4c** and **4d**). These data indicate that a minimum concentration of SP-B between 0 and 0.1 wt% is required to promote gene silencing. Remarkably, as little as 0.2 wt% of SP-B resulted in maximal silencing under the given experimental conditions, further highlighting its potency.

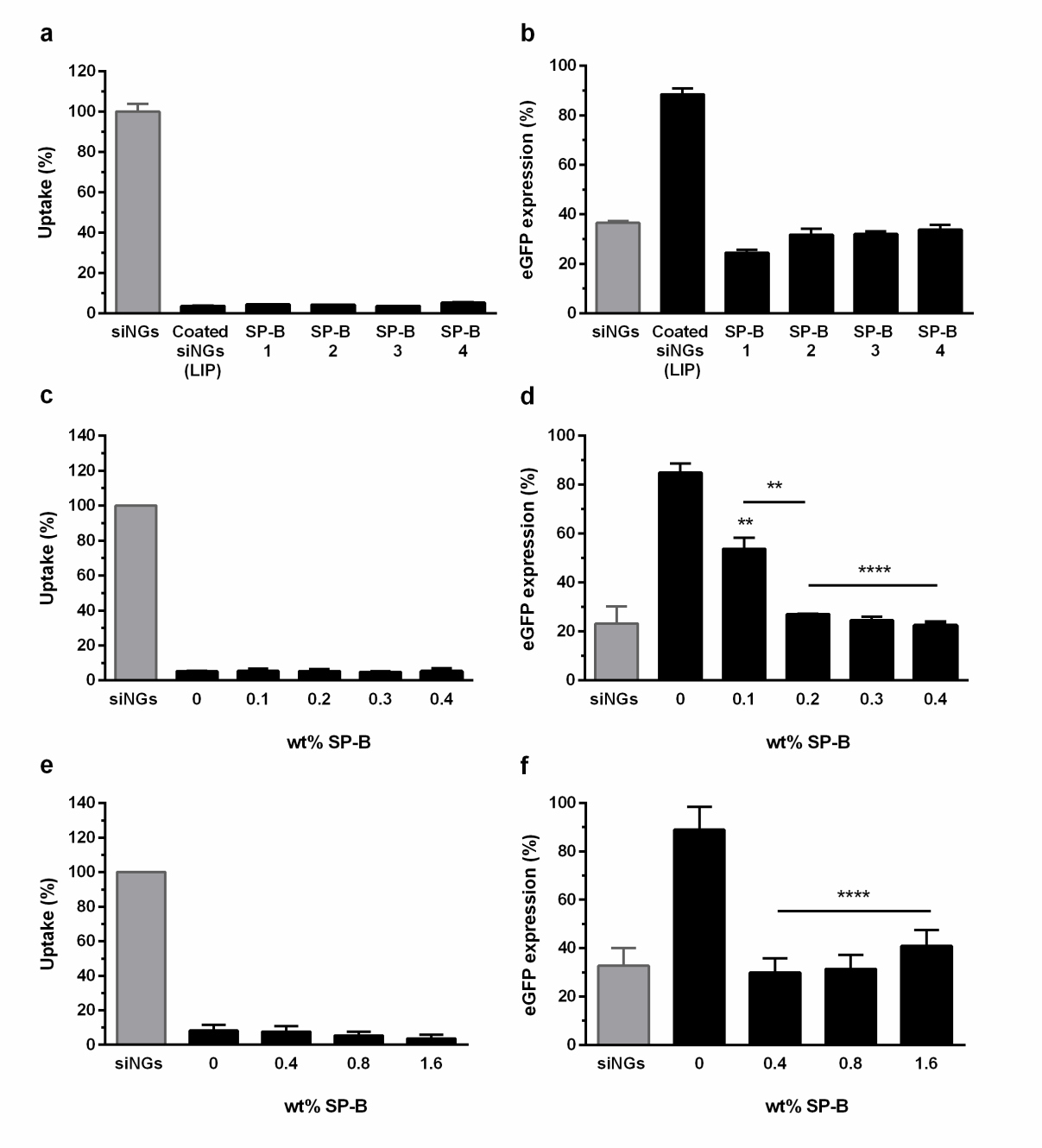

Figure 4. Impact of SP-B source and concentration on the biological activity of the proteolipid coated siNGs. Evaluation of **(a)** cellular uptake and **(b)** gene silencing potential of coated siNGs incorporating SP-B isolated from different sources. The siNGs were layered with DOPC:eggPG (85:15 wt%). SP-B (0.4 wt%) isolated from 3 different native porcine lungs (SP-B 1; SP-B 2; SP-B 3) or isolated from Curosurf® (SP-B 4) was incorporated in the outer lipid layer (technical triplicate). Evaluation of **(c)**,**(e)** cellular uptake and **(d)**,**(f)** gene silencing potential of coated siNGs incorporating different concentrations of SP-B. The siNGs were layered with DOPC:eggPG (85:15 wt%) and SP-B isolated from native porcine lungs. In the uptake experiments, NGs were loaded with fluorescently labeled siRNA (siCy5), for which values of the coated formulations are shown relative to the maximal amount of particles taken up, i.e. for uncoated siNGs (100 %). The eGFP expression was normalized to the expression of cells treated with control siRNA (siCTRL). All experiments were performed with a fixed NG concentration (30 µg/mL) and siRNA concentration (10 nM) (c,d: n=2; e,f: n=4; ** $p \leq 0.01$, **** $p \leq 0.0001$).

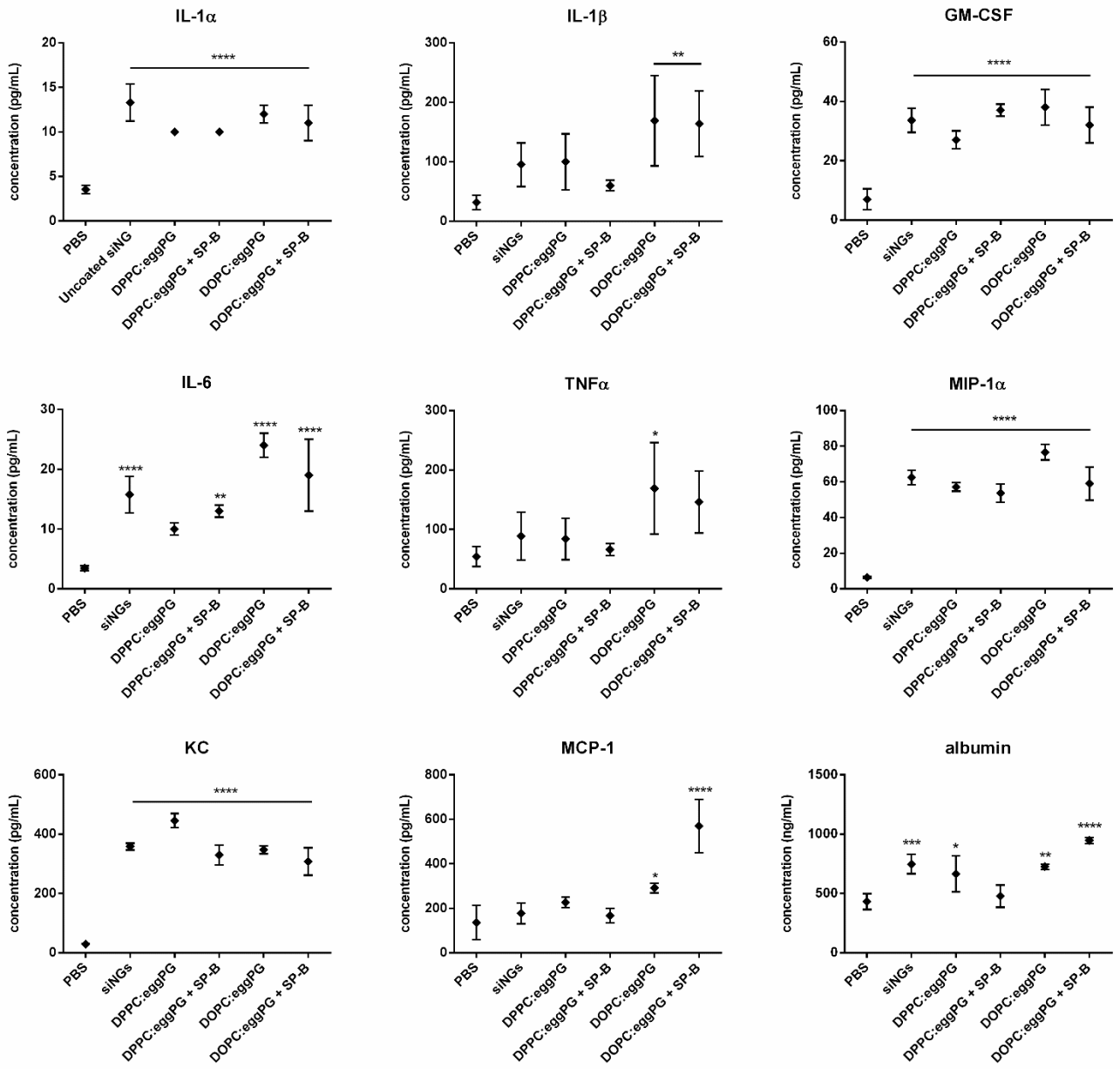

Figure 5. Evaluation of cytokine, chemokine and albumin levels upon administration of different NP compositions. Different NPs were administered to naive BALB/c mice and after 24 h, BAL was extracted and tested for IL-1α, IL-1β, GM-CSF, IL-6, TNFα, MIP-1α, KC and MCP-1 *via* multiplex analysis and albumin *via* ELISA (n=4, all NP values were compared to PBS; * $p \leq 0.05$, ** $p \leq 0.01$, *** $p \leq 0.001$, **** $p \leq 0.0001$).

.

3.4. *In vivo* toxicity of proteolipid coated siNGs in naive BALB/c mice

Following our promising *in vitro* results, we aimed to assess whether the enhanced intracellular siRNA delivery by SP-B in proteolipid coated siNGs could be reproduced *in vivo*.

Since pulmonary administration of nanoparticles (NPs) can induce inflammation, it is of particular interest to first evaluate the possible pro-inflammatory effects of NPs following inhalation therapy. To this end, the levels of distinct cyto- and chemokines were quantified in bronchoalveolar lavage (BAL) fluid of naive, specific pathogen free housed BALB/c mice that had been treated with the different NPs *via* tracheal aspiration.

Compared to PBS treatment, all formulations significantly induced secretion of IL-1α, GM-CSF, IL-6, MIP-1α and KC, whereas for IL-1β, TNFα and MCP-1 this was only the case for one or both DOPC-containing formulations, suggesting a minor inflammatory response due to a phospholipid imbalance in the murine surfactant by administration of the non-endogenous DOPC (**Figure 5**). Indeed, it is known that the surfactant lipid composition plays an important role in many processes at the host-environment interface, including pulmonary inflammation. [38] However, the measured levels for IL-6 and TNFα compared to PBS were not correlated with excessive inflammation according to the literature. [25, 26] The cellular infiltrate in BAL fluid following NP administration did not reveal major differences between the formulations and PBS treated control mice. As expected, alveolar macrophages were the predominant cell type occurring in the BAL (**Figure S5**). All formulations except the siNGs coated with a mixture of DPPC, eggPG and SP-B significantly elevated albumin levels, which is used as a measure of inflammation-associated capillary permeabilization. The highest albumin levels were detected for mice treated with siNGs coated with an SP-B supplemented DOPC:eggPG coat, which is in line with the reduced cell viability observed for this formulation *in vitro* (**Figure S4**). Nevertheless, the maximally measured 2-fold increase compared to PBS is indicative of an acceptable degree of toxicity. [27] Importantly, when combining DPPC with SP-B as proteolipid coat, no elevated albumin levels were detected. Altogether, these data indicate that selecting a formulation that more closely mimics the endogenous surfactant composition is preferred from a toxicological point of view.

3.5. *In vivo* uptake of proteolipid coated siNGs by respiratory immune cells in naive BALB/c mice

Next, it was evaluated to what extent the nanocomposites were internalized by respiratory immune cells following tracheal aspiration in naive mice. The vast majority of Cy5-labeled siRNA delivered by

NPs is taken up by resident alveolar macrophages (rAMs), neutrophils and eosinophils, while little Cy5 fluorescence was detected in T cells. Of note, in stark contrast to our *in vitro* observations, (proteo)lipid coating did not reduce cellular uptake, which however mirrors our earlier findings with Curosurf®-coated siNGs. [10]

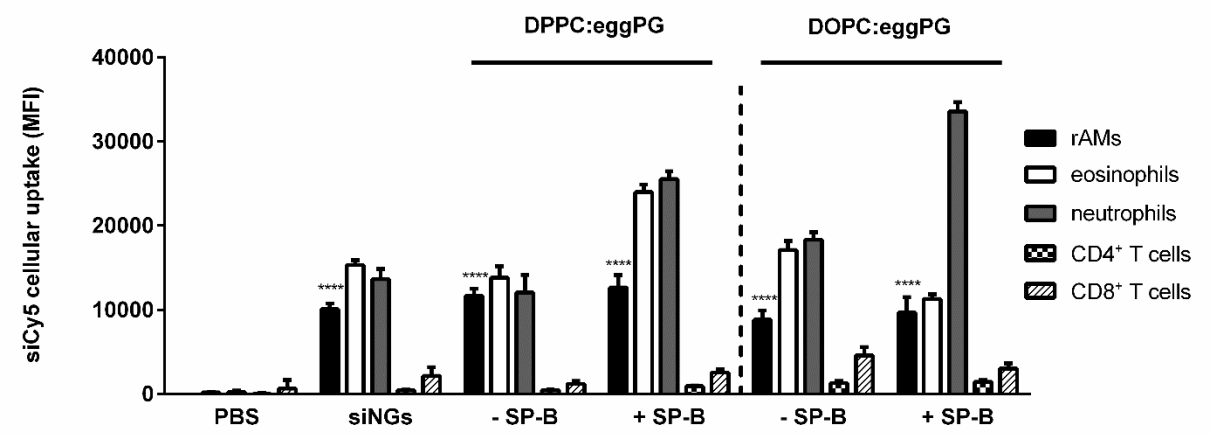

Figure 6. *In vivo* siCy5 delivery to different respiratory immune cells. Resident alveolar macrophages (rAMs), eosinophils, neutrophils, $CD4^+$ T cells and $CD8^+$ T cells were evaluated for geometric mean fluorescence intensity (MFI), 24 h after treatment with a fixed NG dose (100 µg) loaded with 1 pmol siCy5 per µg NGs and coated with different proteolipid compositions (n=4, all siCy5 uptake values for rAMs were compared to PBS; **** $p \leq 0.0001$).

3.6. TNFα silencing in a murine lipopolysaccharide-induced acute lung injury model

It was shown previously that (Curosurf®-coated) siNGs are able to transfect rAMs and induce sequence-specific knockdown of an endogenous target. [18] Given the predominance of rAMs and the high and equivalent uptake by this cell type observed for all NPs independent of the proteolipid coat, a murine lipopolysaccharide (LPS)-induced acute lung injury (ALI) model was chosen to evaluate the impact of SP-B in a phospholipid type coating on *in vivo* siRNA delivery. In ALI, rAMs play a central role in pulmonary inflammation, in particular through their induced secretion of TNFα as an early mediator of the underlying immunologic cascade. [28-30] It has been shown by several groups that downregulation of TNFα in the microenvironment of the lung is indeed associated with reduced lung injury caused by ALI, highlighting its value as a target for therapeutic intervention. [4],[31] Naive BALB/c mice were prophylactically treated with the different NP formulations loaded with a TNFα targeting siRNA (siTNFα), 24 h prior to stimulation with LPS *via* tracheal aspiration (**Figure 7a**). LPS exposure increased TNFα levels >20-fold compared to PBS control and NP administration in naive BALB/c mice (**Figure S6** and **Figure 5**).

Remarkably, in contrast to our *in vitro* observations that were based on eGFP silencing in an H1299_eGFP cell line, no TNFα knockdown could be measured for uncoated siNGs or siNGs layered with an SP-B embedding DOPC:eggPG coat (**Figure 7b**). Although the more rigid DPPC:eggPG coat was less efficient in promoting siRNA delivery *in vitro*, only this formulation was able to reduce the relative TNFα levels in BAL of LPS exposed mice when supplemented with SP-B.

Importantly, the formulation with DPPC as main phospholipid was also best tolerated following *in vivo* administration (**Figure 5**). Differences in NP stability in the lung extracellular fluid, more specifically lipid mixing of the more fluid DOPC composed proteolipid shell with the endogenous surfactant, as well as differences in the intracellular processing of the coated formulations in primary

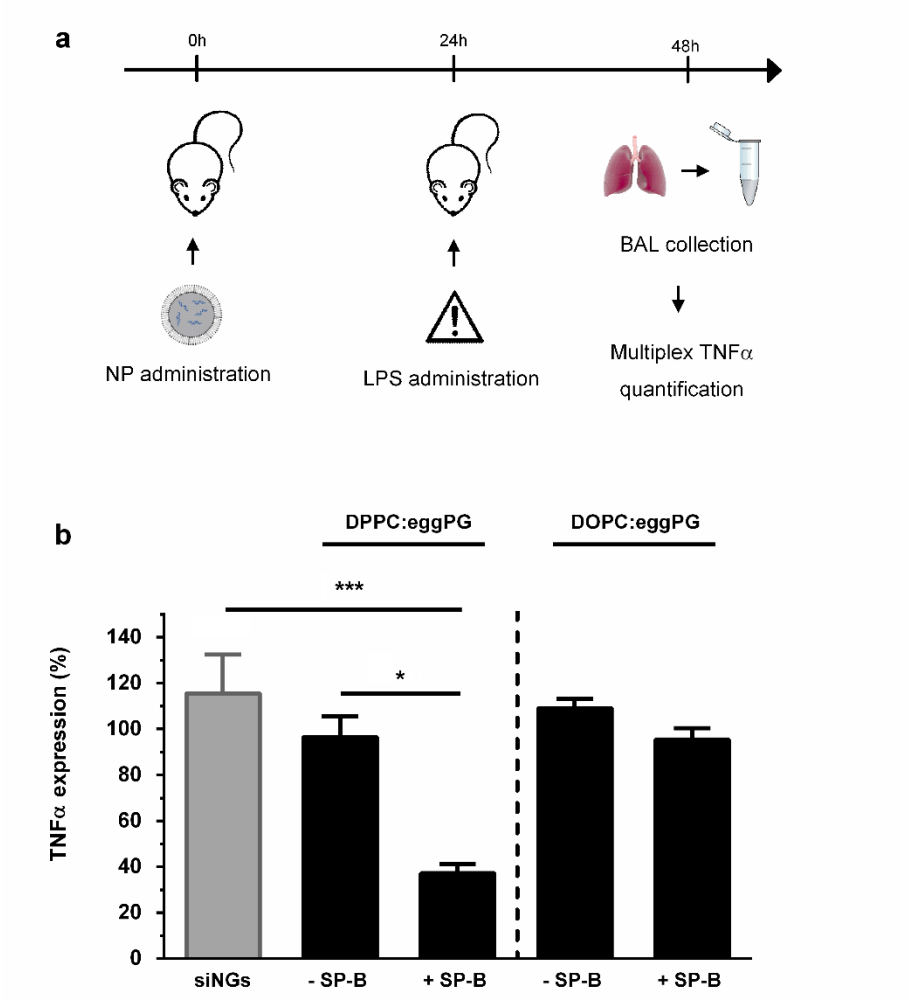

Figure 7. Relative TNFα silencing in a murine acute lung injury (ALI) model. (a) Schematic representation of the executed experiment. **(b)** TNFα levels were quantified in BAL fluid extracted 24 h after LPS stimulation and thus 48 h after instillation of different siCTRL and siTNFα loaded NPs. The TNFα levels obtained with siTNFα loaded siNGs was normalized to the levels in BAL of mice that had received control siRNA (siCTRL). Mice were treated with a fixed NG dose (100 µg) loaded with 1 pmol siTNFα or siCTRL per µg NG (n=4; * $p \leq 0.05$, *** $p \leq 0.001$).

alveolar macrophages, could explain the observed lack of *in vitro-in vivo* correlation regarding the optimal phospholipid composition, although this needs further experimental clarification. Most importantly, in line with our *in vitro* results, we were able to demonstrate that inclusion of SP-B in the particle proteolipid coating is also required for detectable sequence-specific silencing of TNFα.

Of note, in this ALI model absolute TNFα levels for most NPs were found to be equal to or exceed the value for PBS treated mice as shown in **Figure S6**, reducing the intrinsic therapeutic value of these formulations in this particular model. Only the DPPC:eggPG coated formulation containing active siRNA and SP-B reduced TNFα levels with 20% compared to PBS control. The observed TNFα upregulation might indicate that ALI mice are more susceptible to NP-induced effects, as opposed to naive mice. Along with increased neutrophil influx and granulocyte chemotaxis, it has been shown that inhalation of some NPs by LPS-exposed mice indeed can be associated with elevated TNFα levels and in general aggravation of inflammation. The latter underscores the importance of finding the optimal balance between NP-mediated drug delivery and NP-induced off-target effects. [32] In this context, further histopathological scoring of inflammation could add valuable information on the actual toxicity and overall therapeutic benefit of the therapy.

4. CONCLUSIONS

We have identified surfactant protein B (SP-B) as a naturally-derived siRNA delivery enhancer when reconstituted in proteolipid coated siRNA loaded nanogels (siNGs). The beneficial effect of SP-B on siRNA delivery and resulting gene silencing could be observed in an *in vitro* lung epithelial cell line and *in vivo* in a lipopolysaccharide-induced acute lung injury model (ALI), targeting resident alveolar macrophages, albeit that a distinct phospholipid composition was required. The successful proof-of-concept data presented here could pave the way for evaluation of the SP-B delivery platform for therapeutic intervention in various pulmonary pathologies or for identification of key molecular drug targets. Future work will evaluate the presented SP-B centered delivery platform in distinct models of pulmonary pathologies, with careful assessment of NP-induced inflammation to maximize therapeutic benefit.

5. ACKNOWLEDGEMENTS

PM is a doctoral fellow of the Research Foundation Flanders (FWO Vlaanderen) with financial support of the Flanders Innovation and Entrepreneurship Agency (VLAIO). LDB is a postdoctoral researcher of the Special Research Fund of Ghent University. LVH is a junior research assistant of the Department of Biomedical Molecular Biology of Ghent University. RG is an early stage researcher of the NANOMED project, which has received funding from the European Union's Horizon 2020 Research and Innovation Programme Marie Skłodowska Curie Innovative Training Networks (ITN) under grant number 676137. JPG, ME and BO acknowledge support of grants from the Spanish Ministry of Economy (BIO2015-67930-R) and the Regional Government of Madrid (S2013/MIT-2807). SDS and KR gratefully acknowledge FWO Vlaanderen (1517516N), Ghent University (BOF12/GOA/014) and the Agency for Innovation by Science and Technology Flanders (IWT Vlaanderen) (SBO 140061).

6. REFERENCES

1. WHO-The top 10 causes of death. http://www.who.int (accessed 2015 Jul 10).

2. Davidson, B. L.; McCray, P. B. Current prospects for RNA interference-based therapies. *Nat. Rev. Genet.* **2011**, 12, 329-340.

3. Wittrup, A.; Lieberman, J. Knocking down disease: a progress report on siRNA therapeutics. *Nat. Rev. Genet.* **2015**, 16, 543-52.

4. Qiu, Y.; Lam, J. K.; Leung, S. W.; Liang, W. Delivery of RNAi Therapeutics to the Airways-From Bench to Bedside. *Molecules* **2016**, 21.

5. De Backer, L.; Cerrada, A.; Perez-Gil, J.; De Smedt, S. C.; Raemdonck, K. Bio-inspired materials in drug delivery: Exploring the role of pulmonary surfactant in siRNA inhalation therapy. *J. Controlled Release* **2015**, 220, 642-50.

6. Hadinoto, K.; Sundaresan, A.; Cheow, W. S. Lipid-polymer hybrid nanoparticles as a new generation therapeutic delivery platform: a review. *Eur. J. Pharm. Biopharm.* **2013**, 85, 427-43.

7. Mandal, B.; Bhattacharjee, H.; Mittal, N.; Sah, H.; Balabathula, P.; Thoma, L. A.; Wood, G. C. Core-shell-type lipid-polymer hybrid nanoparticles as a drug delivery platform. *Nanomedicine (N.Y., NY, U.S.)* **2013**, 9, 474-91.

8. Raemdonck, K.; Braeckmans, K.; Demeester, J.; De Smedt, S. C. Merging the best of both worlds: hybrid lipid-enveloped matrix nanocomposites in drug delivery. *Chem. Soc. Rev.* **2014**, 43, 444-72.

9. De Backer, L.; Braeckmans, K.; Stuart, M. C.; Demeester, J.; De Smedt, S. C.; Raemdonck, K. Bio-inspired pulmonary surfactant-modified nanogels: A promising siRNA delivery system. *J. Controlled Release* **2015**, 206, 177-86.

10. De Backer, L.; Naessens, T.; De Koker, S.; Zagato, E.; Demeester, J.; Grooten, J.; De Smedt, S. C.; Raemdonck, K. Hybrid pulmonary surfactant-coated nanogels mediate efficient *in vivo* delivery of siRNA to murine alveolar macrophages. *J. Controlled Release* **2015**, 217, 53-63.

11. Raemdonck, K.; Naeye, B.; Buyens, K.; Vandenbroucke, R. E.; Hogset, A.; Demeester, J.; De Smedt, S. C. Biodegradable Dextran Nanogels for RNA Interference: Focusing on Endosomal Escape and Intracellular siRNA Delivery. *Adv. Funct. Mater.* **2009**, 19, 1406-1415.

12. Raemdonck, K.; Naeye, B.; Hogset, A.; Demeester, J.; De Smedt, S. C. Prolonged gene silencing by combining siRNA nanogels and photochemical internalization. *J. Controlled Release* **2010**, 145, 281-288.

13. Naeye, B.; Raemdonck, K.; Remaut, K.; Sproat, B.; Demeester, J.; De Smedt, S. C. PEGylation of biodegradable dextran nanogels for siRNA delivery. *Eur. J. Pharm. Sci.* **2010**, 40, 342-351.

14. Balmert, S. C.; Little, S. R. Biomimetic delivery with micro- and nanoparticles. *Adv. Mater. (Weinheim, Ger.)* **2012**, 24, 3757-78.

15. Yoo, J. W.; Irvine, D. J.; Discher, D. E.; Mitragotri, S. Bio-inspired, bioengineered and biomimetic drug delivery carriers. *Nat. Rev. Drug Discovery* **2011**, 10, 521-535.

16. Lopez-Rodriguez, E.; Perez-Gil, J. Structure-function relationships in pulmonary surfactant membranes: from biophysics to therapy. *Biochim. Biophys. Acta* **2014**, 1838, 1568-85.

17. Blanco, O.; Perez-Gil, J. Biochemical and pharmacological differences between preparations of exogenous natural surfactant used to treat Respiratory Distress Syndrome: Role of the different components in an efficient pulmonary surfactant. *Eur. J. Pharmacol.* **2007**, 568, 1-15.

18. Zhang, H.; Fan, Q.; Wang, Y. E.; Neal, C. R.; Zuo, Y. Y. Comparative study of clinical pulmonary surfactants using atomic force microscopy. *Biochim. Biophys. Acta* **2011**, 1808, 1832-42.

19. De Backer, L.; Braeckmans, K.; Demeester, J.; De Smedt, S. C.; Raemdonck, K. The influence of natural pulmonary surfactant on the efficacy of siRNA-loaded dextran nanogels. *Nanomedicine (London, U.K.)* **2013**, 8, 1625-1638.

20. Ryan, M. A.; Qi, X. Y.; Serrano, A. G.; Ikegami, M.; Perez-Gil, J.; Johansson, J.; Weaver, T. E. Mapping and analysis of the lytic and fusogenic domains of surfactant protein B. *Biochemistry* **2005**, 44, 861-872.

21. Parra, E.; Alcaraz, A.; Cruz, A.; Aguilella, V. M.; Perez-Gil, J. Hydrophobic Pulmonary Surfactant Proteins SP-B and SP-C Induce Pore Formation in Planar Lipid Membranes: Evidence for Proteolipid Pores. *Biophys. J.* **2013**, 104, 146-155.

22. Frey, S. L.; Pocivavsek, L.; Waring, A. J.; Walther, F. J.; Hernandez-Juviel, J. M.; Ruchala, P.; Lee, K. Y. Functional importance of the NH2-terminal insertion sequence of lung surfactant protein B. *Am. J. Physiol. Lung Cell Mol. Physiol.* **2010**, 298, L335-47.

23. Keating, E.; Zuo, Y. Y.; Tadayyon, S. M.; Petersen, N. O.; Possmayer, F.; Veldhuizen, R. A. A modified squeeze-out mechanism for generating high surface pressures with pulmonary surfactant. *Biochim. Biophys. Acta* **2012**, 1818, 1225-34.

24. Olmeda, B.; Garcia-Alvarez, B.; Gomez, M. J.; Martinez-Calle, M.; Cruz, A.; Perez-Gil, J. A model for the structure and mechanism of action of pulmonary surfactant protein B. *FASEB J.* **2015**.

25. Johansson, E.; Boivin, G. P.; Yadav, J. S. Early immunopathological events in acute model of mycobacterial hypersensitivity pneumonitis in mice. *J. Immunotoxicol.* **2017**, 14, 77-88.

26. Aragao-Santiago, L.; Hillaireau, H.; Grabowski, N.; Mura, S.; Nascimento, T. L.; Dufort, S.; Coll, J. L.; Tsapis, N.; Fattal, E. Compared *in vivo* toxicity in mice of lung delivered biodegradable and non-biodegradable nanoparticles. *Nanotoxicology* **2016**, 10, 292-302.

27. Chen, S. S.; Yin, Z. F.; Chen, T.; Qiu, H.; Wei, Y. R.; Du, S. S.; Jin, Y. P.; Zhao, M. M.; Wu, Q.; Weng, D.; Li, H. P. Development of a non-infectious rat model of acute exacerbation of idiopathic pulmonary fibrosis. *J. Thorac. Dis.* **2017**, 9, 96-105.

28. Okamoto, T.; Gohil, K.; Finkelstein, E. I.; Bove, P.; Akaike, T.; van der Vliet, A. Multiple contributing roles for NOS2 in LPS-induced acute airway inflammation in mice. *Am. J. Physiol. Lung Cell Mol. Physiol.* **2004**, 286, L198-209.

29. Johnson, E. R.; Matthay, M. A. Acute lung injury: epidemiology, pathogenesis, and treatment. *J. Aerosol Med. Pulm. Drug Deliv.* **2010**, 23, 243-52.

30. Mukhopadhyay, S.; Hoidal, J. R.; Mukherjee, T. K. Role of TNFalpha in pulmonary pathophysiology. *Respir. Res.* **2006**, 7, 125.

31. Bittencourt-Mernak, M. I.; Pinheiro, N. M.; Santana, F. P.; Guerreiro, M. P.; Saraiva-Romanholo, B. M.; Grecco, S. S.; Caperuto, L. C.; Felizardo, R. J.; Camara, N. O.; Calvo Tiberio, I. F.; Martins, M. A.; Lago, J. H.; Prado, C. M. Prophylactic and therapeutic treatment with flavonone sakuranetin ameliorates LPS-induced acute lung injury. *Am. J. Physiol. Lung Cell Mol. Physiol.* **2016**, ajplung 00444 2015.

32. Inoue, K.; Takano, H.; Yanagisawa, R.; Hirano, S.; Kobayashi, T.; Fujitani, Y.; Shimada, A.; Yoshikawa, T. Effects of inhaled nanoparticles on acute lung injury induced by lipopolysaccharide in mice. *Toxicology* **2007**, 238, 99-110.

33. vanDijkWolthuis, W. N. E.; Tsang, S. K. Y.; KettenesvandenBosch, J. J.; Hennink, W. E. A new class of polymerizable dextrans with hydrolyzable groups: hydroxyethyl methacrylated dextran with and without oligolactate spacer. *Polymer* **1997**, 38, 6235-6242.

34. Pérez-Gil, J.; Cruz, A.; Casals, C. Solubility of Hydrophobic Surfactant Proteins in Organic-Solvent Water Mixtures - Structural Studies on Sp-B and Sp-C in Aqueous-Organic Solvents and Lipids. *Biochim. Biophys. Acta* **1993**, 1168, 261-270.

35. Rouser, G.; Siakotos, A. N.; Fleische.S. Quantitative Analysis of Phospholipids by Thin-Layer Chromatography and Phosphorus Analysis of Spots. *Lipids* **1966**, 1, 85-&.

36. Rao, G. V.; Tinkle, S.; Weissman, D. N.; Antonini, J. M.; Kashon, M. L.; Salmen, R.; Battelli, L. A.; Willard, P. A.; Hoover, M. D.; Hubbs, A. F. Efficacy of a technique for exposing the mouse lung to particles aspirated from the pharynx. *J. Toxicol. Environ. Health A* **2003**, 66, 1441-52.

37. Van Hoecke, L.; Job, E. R.; Saelens, X.; Roose, K. Bronchoalveolar Lavage of Murine Lungs to Analyze Inflammatory Cell Infiltration. *J Vis Exp* (123) **2017**.

38. Fessler, M.B.; Summer R.S. Surfactant Lipids at the Host-Environment Interface: Metabolic Sensors, Suppressors, and Effectors of Inflammatory Lung Disease. *Am J Respir Cell Mol Biol* **2016**, 624-635

7. SUPPLEMENTARY

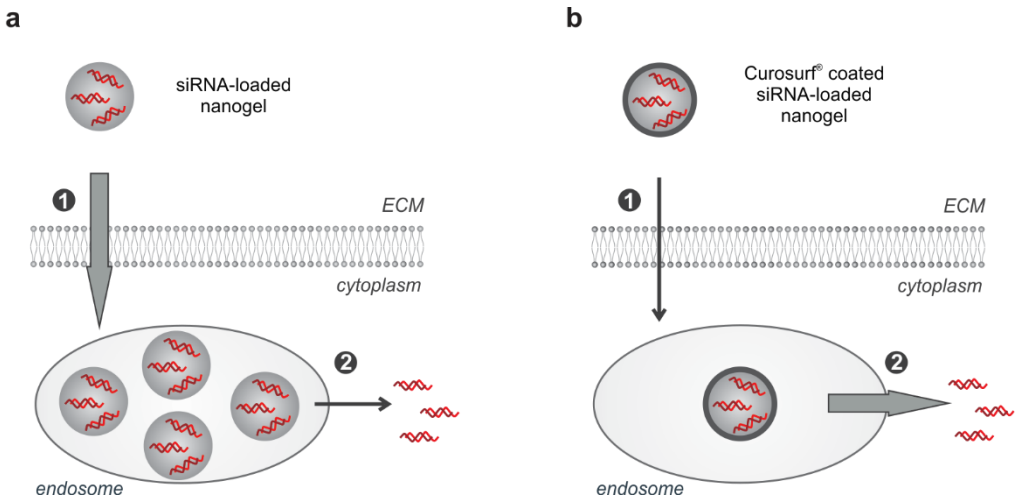

Scheme S1. Graphical representation of the siRNA delivery efficacy guided by (a) siRNA-loaded nanogels and (b) Curosurf® coated siRNA-loaded nanogels. As reported previously, [9] the **(1)** cellular internalization of the nanogels is significantly reduced in the presence of a Curosurf® outer layer. Remarkably, despite poor intracellular siRNA uptake, the **(2)** gene silencing potential was maintained, suggesting that the Curosurf® outer layer promotes the cytosolic delivery of siRNA e.g. through improved endosomal escape. In this work, we aim to identify the molecular components in Curosurf® responsible for this enhanced delivery. ECM: extracellular matrix.

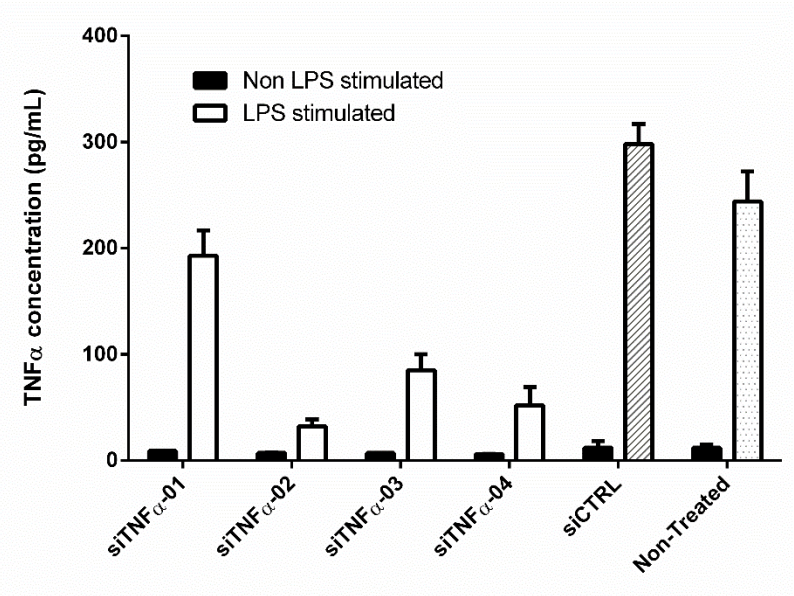

Figure S1. ***In vitro*** **TNFα knockdown by a siTNFα set of four in (LPS stimulated) MH-S cells.** All experiments were performed with a fixed NG concentration (60 µg/mL) and siRNA concentration (20 nM) (technical triplicate). siTNFα-02 was selected for further experiments.

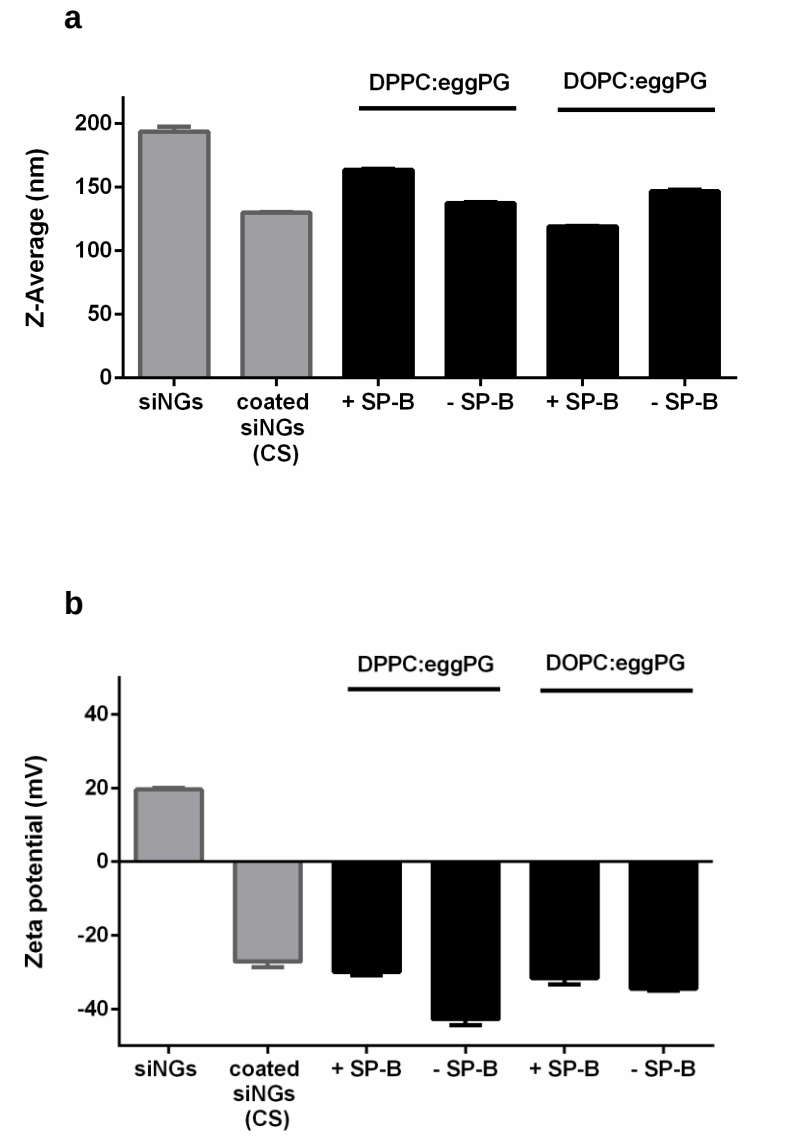

Figure S2. (a) Hydrodynamic diameter and (b) zeta potential of (coated) nanogel (NG) formulations as measured by Dynamic Light Scattering (DLS). All particles were prepared under the same experimental conditions as those used for *in vitro* and *in vivo* experiments. Measurements were performed at room temperature in HEPES buffer (pH 7.4, 20 mM). PDI for all samples was between 0.2 and 0.25 (*n*=3).

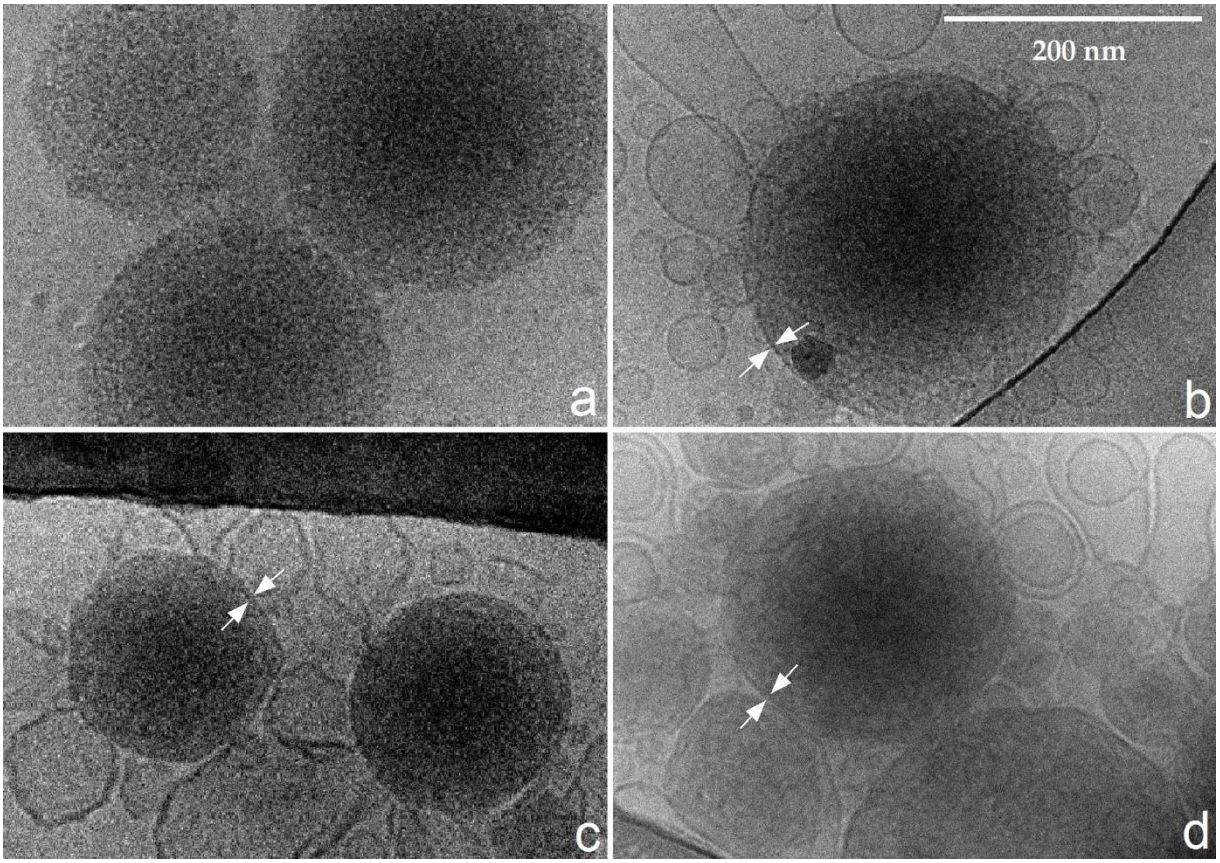

Figure S3. Transmission electron cryomicroscopy images of different nanoformulations. The figure shows a comparison of (**a**) uncoated; (**b**) Curosurf® coated; (**c**) DPPC:eggPG:SP-B coated and (**d**) DOPC:eggPG:SP-B coated siRNA-loaded nanogels (siNGs). The white arrows mark the proteolipid shell deposited on the surface of the siNG core.

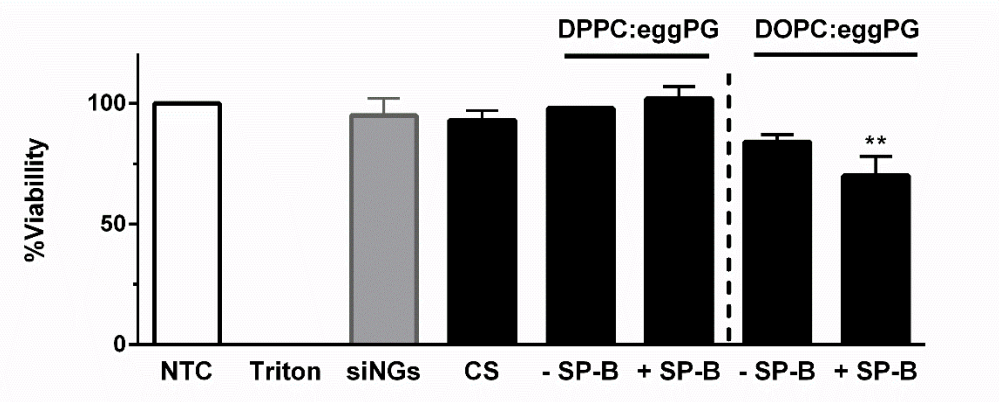

Figure S4. *In vitro* cell viability of different formulations. H1299_eGFP cells were incubated with different NP in the same conditions as uptake and silencing experiments. 24 h after incubation, luminescence was measured per condition via a CellTiter Glo® assay and viability was determined as percentage of luminescent signal relative to non-treated cells (NTC) for each formulation. Treatment with Triton-X100 (Triton) for complete cell lysis was used as a negative control (n=2; ** $p \leq 0.01$).

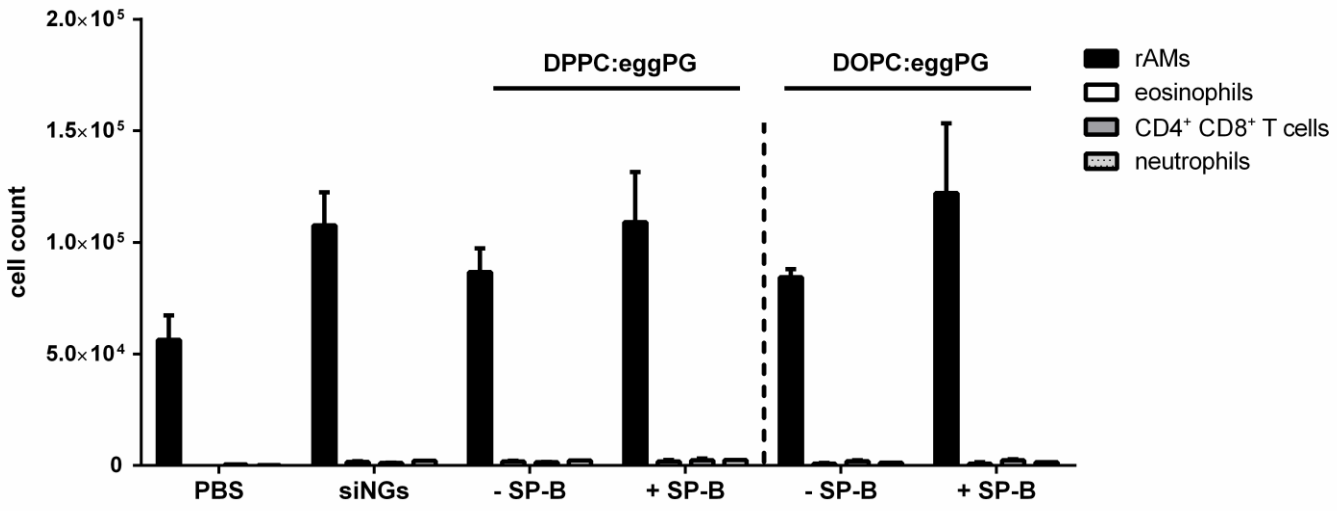

Figure S5. Immune cell infiltration after NP administration in naive BALB/c mice. The cellular fraction of BAL fluid as quantified for resident alveolar macrophages (rAMs), eosinophils, neutrophils, $CD4^+$ T cells and $CD8^+$ T cells *via* flow cytometry, 24 h after treatment with a fixed NG dose (100 µg) loaded with 1 pmol siCy5 per µg NG and coated with different proteolipid compositions (*n*=4).

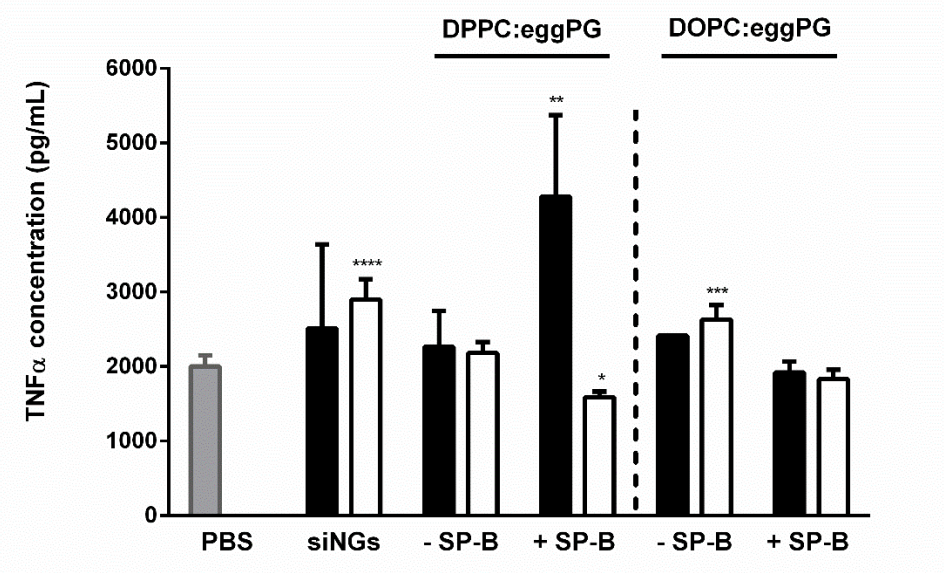

Figure S6. Absolute TNFα levels in a murine acute lung injury (ALI) model. TNFα levels were quantified in BAL fluid extracted 24 h after LPS stimulation and thus 48 h after instillation of different siCTRL (black bars) and siTNFα (white bars) loaded NPs (**Figure 7a**). Mice were treated with a fixed NG dose (100 µg) loaded with 1 pmol siTNFα or siCTRL per µg NG. PBS was administered as a control (grey bar) (n=4, all NP values were compared to PBS; * $p \leq 0.05$, ** $p \leq 0.01$, *** $p \leq 0.001$, **** $p \leq 0.0001$).

Table S1. Overview of compositions of different proteolipid coating mixtures for siNGs. All numbers are expressed as wt% of the total mixture.

	DPPC	DOPC	POPC	eggPG	SP-B	SP-C	Figure
DPPC:POPC:eggPG	50		35	15			1
DPPC:POPC:eggPG + SP-B	49.8		34.86	14.94	0.4		1
DPPC:POPC:eggPG + SP-C	49.65		34.76	14.9		0.7	1
DPPC:POPC:eggPG + SP-B + SP-C	49.45		34.62	14.84	0.4	0.7	1
DPPC:eggPG	85			15			2,5,6,7
DOPC:eggPG		85		15			2,3,4,5,6,7
DPPC:eggPG + SP-B	84.66			14.94	0.4		5,6,7
DPPC:eggPG + SP-B (0.8 wt%)	84.32			14.88	0.8		2
DOPC:eggPG + SP-B		84.66		14.94	0.4		3,4,5,6,7
DOPC:eggPG + SP-C		84.41		14.9		0.7	3
DOPC:eggPG + SP-B + SP-C		84.07		14.84	0.4	0.7	3
DOPC:eggPG + SP-B (0.1 wt%)		84.92		14.99	0.1		4
DOPC:eggPG + SP-B (0.2 wt%)		84.83		14.97	0.2		4
DOPC:eggPG + SP-B (0.3 wt%)		84.75		14.96	0.3		4
DOPC:eggPG + SP-B (0.8 wt%)		84.32		14.88	0.8		2,4
DOPC:eggPG + SP-B (1.6 wt%)		83.64		14.76	1.6		4